Particle escapes in an open quantum network via multiple leads

Tooru Taniguchi and Shin-ichi Sawada
School of Science and Technology, Kwansei Gakuin University, 2-1 Gakuen, Sanda City, Japan
(Received 5 August 2011; published 9 December 2011)

Quantum escape of a particle from an end of a one-dimensional finite region to N semi-infinite leads is discussed from a scattering theory approach. Depending on the potential barrier amplitude at the junction, the probability $P(t)$ for a particle to remain in the finite region at time t shows two different decay behaviors at long times; one is proportional to N^2/t^3 and another is proportional to $1/(N^2 t)$. In addition, the velocity $V(t)$ for a particle to leave the finite region, defined from a probability current of the particle position, decays asymptotically as a power of time $\sim 1/t$, independent of the number of leads and the initial wave function. For a finite time, the probability $P(t)$ decays exponentially in time with a smaller decay rate for a greater number of leads, and the velocity $V(t)$ shows a time oscillation whose amplitude is larger for a greater number of leads. Particle escapes from the both ends of a finite region to multiple leads are also discussed using a different boundary condition.

DOI: 10.1103/PhysRevA.84.062707 PACS number(s): 03.65.Nk, 05.30.−d, 73.23.−b

I. INTRODUCTION

The escape of particles is a typical nonequilibrium phenomenon in open systems. It is a current of particles from a region where the particles were initially confined. The concept of escape has been used to describe a variety of physical phenomena, such as the α decay of a nucleus [1–3], chemical reactions such as the Kramers' escape problem [4–6], and so on. Some dynamical properties, like chaos [7–9], the recurrence time [10], the first-passage time [5,6], transport coefficients [11–13], etc., have also been investigated via the escape behavior of particles. Particle escapes have been discussed in many types of systems, for example, stochastic systems [4–6], classical billiard systems [7,8,14–16], maps [9,10,17], and quantum systems [1–3,18–22].

Escape phenomena in open systems cause a decay of various quantities due to the particle current from the region. For instance, the probability for particles to remain in the initially confined region, which we call the survival probability in this paper, would decay in time, if particles continue to flow out from the initial region. Such decay properties in escape systems have led to some interesting results and hypotheses. For example, in classical mechanical systems with a particle escape via a small hole, the survival probability would decay exponentially in time if the dynamics is chaotic, while it would decay as a power for nonchaotic systems [7–10,15]. On the other hand, in many quantum-mechanical systems, the survival probability decays as a power asymptotically in time [3,18,20,22–24] with an exponential decay for a finite time [3,20,22,23], and values of the power of the decay vary due to initial conditions [25] or particle interactions [26–28], and so on.

In this paper we discuss particle escape in quantum-mechanical networks as an example of open dynamical systems. The quantum network system is also called the "quantum graph" and is constructed by connecting finite and infinite narrow wires like a network. It also has been widely used as a model to describe mesoscopic transport such as Aharonov-Bohm types of effects [29,30], resonance tunnellings [31,32], current splitters [33–36], chaos and diffusion [37,38], and so on. Steady electric currents in open quantum network systems are described by quantum scattering theory [39–42]. This kind of quantum system with narrow wires could be realized experimentally as a combination of atomic or molecular wires or as a graphlike structure on the surface of a semiconductor using recent developments in nanotechnology [43–45].

An important feature of network systems is the effect of a current splitter at a network junction. In order to consider such a splitting effect of currents in quantum escapes as simple and concrete as possible, we consider particle escapes from a finite one-dimensional region with a length L via N semi-infinite one-dimensional leads. The multiple leads are connected at one end of the finite region with a potential barrier of amplitude Λ at the junction, and we impose a fixed boundary condition at another end of the finite region. We use quantum scattering as an analytical method of describing particle escape in such a quantum network, and we consider the decay properties of two quantities that characterize the quantum escape. The first decaying quantity is the survival probability $P(t)$ for the particle to remain in the finite region at time t. We show analytically that after a long time the survival probability $P(t)$ depends on the number of attached semi-infinite leads as the N^2, i.e., $\lim_{t\to+\infty} P(t)/[P(t)|_{N=1}] = N^2$, for $\Lambda \neq -\hbar^2/(2mL)$ (where m is the mass of the particle and $2\pi\hbar$ is Planck's constant). This means that at long times the particle has a larger survival probability by connecting more semi-infinite leads. Moreover, in this case, the survival probability $P(t)$ decays as a power $\sim 1/t^3$ at long times. In contrast, in the case of $\Lambda = -\hbar^2/(2mL)$ we obtain a N^{-2} ratio $\lim_{t\to+\infty} P(t)/[P(t)|_{N=1}] = 1/N^2$ for the survival probability $P(t)$, meaning that after a long time a particle escapes more by connecting more leads. Here, the survival probability $P(t)$ decays as a power $\sim 1/t$ asymptotically in time, differing from the case of $\Lambda \neq -\hbar^2/(2mL)$. We also discuss finite-time properties of the survival probability numerically and show that for a finite time the survival probability decays exponentially for a longer time with a smaller decay rate by connecting more leads. As the second decay quantity to investigate in quantum particle escape, we consider the velocity $V(t)$ for the particle to escape from the finite region, which is introduced by the equation of continuity for the particle position probability. We show analytically that the escape velocity $V(t)$ behaves asymptotically in time as $V(t) \overset{t\to+\infty}{\sim} L/t$ for $\Lambda \neq -\hbar^2/(2mL)$ and $V(t) \overset{t\to+\infty}{\sim} L/(3t)$ for $\Lambda = -\hbar^2/(2mL)$, which are independent of the number N of leads and the initial wave function, and so on. It is also shown by numerical calculations that for a finite time the escape velocity $V(t)$ oscillates in time and takes a larger magnitude for the oscillations for more attached leads. Furthermore, by using a different boundary condition, our scattering approach to quantum network systems also allows us to discuss particle escape from a finite region of length $2L$ with both ends connected to N semi-infinite one-dimensional leads.

The outline of this paper is as follows. In Sec. II, the quantum network system with a finite wire connected to multiple leads is introduced. Based on the equation of continuity for particle position probability, we introduce a probability current whose conservation imposes boundary conditions at the junction of leads and at the terminated end of the finite wire. These boundary conditions specify the scattering states of this system, from which we describe the time evolution of the wave function for the system. In Sec. III, we introduce the survival probability $P(t)$ from the particle position probability and the escape velocity $V(t)$ from the probability current in the quantum network and discuss these decay properties. Finally, we give some conclusions and remarks in Sec. IV.

II. QUANTUM SCATTERING APPROACH TO NETWORK SYSTEMS WITH MULTIPLE LEADS

A. Quantum network system and boundary conditions

We consider quantum network systems consisting of a finite one-dimensional segment with a length L whose end is connected to N semi-infinite one-dimensional leads. (See Fig. 1 as a schematic illustration of this network.) We call the finite segment with the length L the region $\mathcal{L}^{(0)}$ and also call the n-th semi-infinite segment of lead the region $\mathcal{L}^{(n)}$ $(n = 1,2,\ldots,N)$. In each region $\mathcal{L}^{(n)}$ we put the $x^{(n)}$ axis of coordinates with the origin O at the junction of leads, in which the positive direction of the $x^{(n)}$ axis is taken from the origin O to the region $\mathcal{L}^{(n)}$ $(n = 0,1,2,\ldots,N)$.

We introduce the wave function $\Psi^{(n)}(x,t)$ of a particle in this quantum network at time t and position $x \in \mathcal{L}^{(n)}$ for $x > 0$. From the Schrödinger equation for the wave function $\Psi^{(n)}(x,t)$ with a real potential we derive the equation of continuity for the particle position probability density

$$\rho^{(n)}(x,t) \equiv |\Psi^{(n)}(x,t)|^2 \tag{1}$$

as

$$\frac{\partial \rho^{(n)}(x,t)}{\partial t} + \frac{\partial \rho^{(n)}(x,t) v^{(n)}(x,t)}{\partial x} = 0, \tag{2}$$

in which the local velocity $v^{(n)}(x,t)$ at the position $x \in \mathcal{L}^{(n)}$ and the time t is introduced as

$$v^{(n)}(x,t) \equiv \frac{\hbar}{m} \mathrm{Im}\left[\frac{\frac{\partial \Psi^{(n)}(x,t)}{\partial x}}{\Psi^{(n)}(x,t)}\right] \tag{3}$$

with the mass m of particle and Planck's constant $2\pi\hbar$ [46]. Here, $\mathrm{Im}[X]$ means the imaginary part of X for any complex number X.

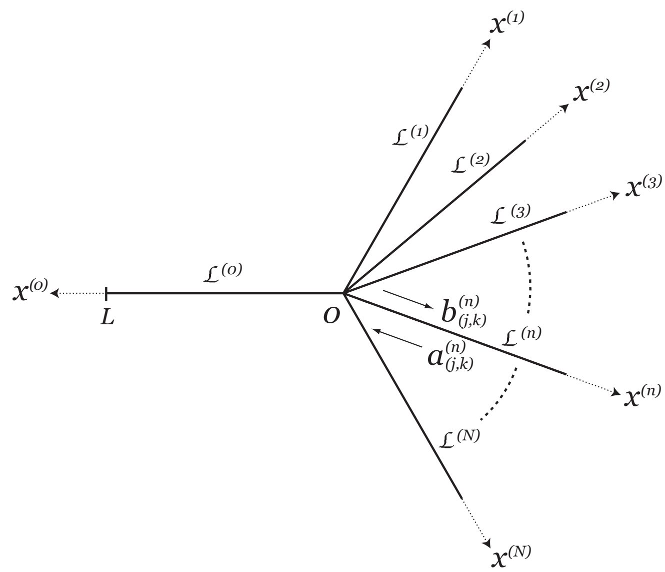

FIG. 1. A quantum network with a junction for multiple leads. It consists of a finite region $\mathcal{L}^{(0)}$ with a length L and the semi-infinite one-dimensional region $\mathcal{L}^{(n)}$ $(n = 1,2,\ldots,N)$ connected to an end of the region $\mathcal{L}^{(0)}$. The $x^{(n)}$ axis of coordinates is taken in the region $\mathcal{L}^{(n)}$ with the origin O at the junction and its coordinate satisfies $x^{(n)} > 0$ $(n = 0,1,2,\ldots,N)$. The coefficient $a^{(n)}_{(j,k)}$ $(b^{(n)}_{(j,k)})$ is the amplitude of the incident wave to (the scattered wave from) the junction in the region $\mathcal{L}^{(n)}$ by use of a plain wave injected from the j-th lead with wave number k.

To describe the quantum state at the junction O, we impose the condition that the wave function of the system is continuous at any position, including at the origin O so the boundary conditions become

$$\Psi(0,t) \equiv \lim_{x\to+0} \Psi^{(0)}(x,t) = \lim_{x\to+0} \Psi^{(1)}(x,t) = \cdots = \lim_{x\to+0} \Psi^{(N)}(x,t) \tag{4}$$

which are satisfied at any time t. We further assume that there is no net particle current source at the junction O, namely $\lim_{x\to+0} \sum_{n=0}^{N} \rho^{(n)}(x,t) v^{(n)}(x,t) = 0$, leading to

$$\lim_{x\to+0} \sum_{n=0}^{N} v^{(n)}(x,t) = 0 \tag{5}$$

for the local velocity [Eq. (3)], noting that from Eq. (4) the position probability density $\lim_{x\to+0} \rho^{(n)}(x,t)$ is independent of the region number n [47]. Using Eqs. (3) and (4), Eq. (5) is rewritten as

$$\lim_{x\to+0} \sum_{n=0}^{N} \frac{\partial \Psi^{(n)}(x,t)}{\partial x} = \lambda \Psi(0,t) \tag{6}$$

with a real constant λ [39,42,48]. It is important to note that for the case of $N = 1$ the condition (6) is equivalent to the boundary condition for a δ-function type of potential with the amplitude $\hbar^2\lambda/(2m)$ in a one-dimensional one-particle system. In this sense, we regard the real constant

$$\Lambda \equiv \frac{\hbar^2 \lambda}{2m} \tag{7}$$

with the constant λ appearing in Eq. (6) as a potential barrier amplitude at the junction O. Finally, we impose the condition that there is no particle current source at the end $x^{(0)} = L$ of the region $\mathcal{L}^{(0)}$, so

$$v^{(0)}(L,t) = 0, \tag{8}$$

namely

$$\left.\frac{\partial \Psi^{(0)}(x,t)}{\partial x}\right|_{x=L} = \mu \Psi^{(0)}(L,t) \tag{9}$$

with a real constant μ, similarly to Eq. (6) [47,48].

B. Scattering states and matrix

We assume that the quantum network introduced in Sec. II A consists of ideal leads, i.e., there is no potential in any part of the region $\mathcal{L}^{(n)}$, $n = 0,1,\dots,N$ except at the junction and at the end $x^{(0)} = L$ of the region $\mathcal{L}^{(0)}$. In this case, the energy eigenstate $\Phi^{(n)}_{(j,k)}(x)$ at the point x in $\mathcal{L}^{(n)}$ is presented by use of a superposition of plain waves with wave number k (>0) as

$$\Phi^{(n)}_{(j,k)}(x) = a^{(n)}_{(j,k)} e^{-ikx} + b^{(n)}_{(j,k)} e^{ikx}, \tag{10}$$

$n = 0,1,\dots,N$, corresponding to the energy eigenvalue $E_k = \hbar^2 k^2/(2m)$. Here, we introduce the suffix j in the quantities $\Phi^{(n)}_{(j,k)}(x)$, $a^{(n)}_{(j,k)}$, and $b^{(n)}_{(j,k)}$ to distinguish different states with the same energy E_k as discussed later in detail. The constants $a^{(n)}_{(j,k)}$ and $b^{(n)}_{(j,k)}$ in Eq. (10) are regarded as the amplitude of the incident wave and the wave scattered from the junction O, respectively. The $(N+1)$-dimensional column vector $\boldsymbol{b}_{(j,k)} \equiv (b^{(0)}_{(j,k)}\ b^{(1)}_{(j,k)}\ \cdots\ b^{(N)}_{(j,k)})^T$ is connected to the $(N+1)$-dimensional column vector $\boldsymbol{a}_{(j,k)} \equiv (a^{(0)}_{(j,k)}\ a^{(1)}_{(j,k)}\ \cdots\ a^{(N)}_{(j,k)})^T$ as

$$\boldsymbol{b}_{(j,k)} = S_k \boldsymbol{a}_{(j,k)} \tag{11}$$

with the scattering matrix S_k. Here, the notation $\boldsymbol{X}^T$ denotes the transpose of $\boldsymbol{X}$ for any vector $\boldsymbol{X}$. In Eq. (11) we suppressed the suffix j for the scattering matrix S_k, because as shown later in Eq. (12) the scattering matrix is independent of the suffix j. The energy eigenstate (10), which has nonzero value even in the infinite region $x^{(n)} \to +\infty$ of $\mathcal{L}^{(n)}$, $n = 1,2,\dots,N$, is the scattering state of the quantum network system.

The scattering state (10) as a special example of the wave function $\Psi^{(n)}(x,t)$ must satisfy the conditions of Eqs. (4) and (6), leading to the specific form of the scattering matrix S_k as

$$S_k = \frac{2}{N+1+i\frac{\lambda}{k}} U - I. \tag{12}$$

Here, I is the $(N+1)\times(N+1)$ identity matrix, and U is the $(N+1)\times(N+1)$ matrix whose elements are all given by 1. [See Appendix A for an derivation of Eq. (11) with the scattering matrix (12).] Noting the relation $U^2 = (N+1)U$, the scattering matrix (12) is shown to be a unitary matrix satisfying the relation

$$S_k^\dagger S_k = S_k S_k^\dagger = I \tag{13}$$

with the Hermitian matrix $S_k^\dagger$ of S_k, supporting the relation $|\boldsymbol{b}_{(j,k)}|^2 = |\boldsymbol{a}_{(j,k)}|^2$ by use of Eq. (11).

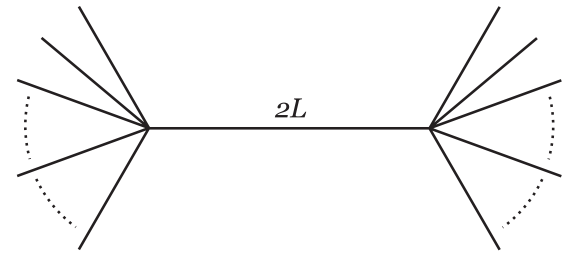

FIG. 2. A quantum network with two junctions for multiple leads at the both ends of the finite region with a length $2L$.

On the other hand, the condition (9) leads to the relation

$$a^{(0)}_{(j,k)} = \frac{1+i\frac{\mu}{k}}{1-i\frac{\mu}{k}} e^{2ikL} b^{(0)}_{(j,k)} \tag{14}$$

between the amplitudes $a^{(0)}_{(j,k)}$ and $b^{(0)}_{(j,k)}$ for the scattering state in the finite region $\mathcal{L}^{(0)}$. The condition (14) guarantees the same magnitude $|b^{(0)}_{(j,k)}|^2 = |a^{(0)}_{(j,k)}|^2$ of the plain waves propagating to the opposite directions with each other in the finite region $\mathcal{L}^{(0)}$. The relation (14) includes two special cases:

$$a^{(0)}_{(j,k)} = -e^{2ikL} b^{(0)}_{(j,k)} \quad \text{for } \mu \to +\infty, \tag{15}$$

$$a^{(0)}_{(j,k)} = +e^{2ikL} b^{(0)}_{(j,k)} \quad \text{for } \mu = 0, \tag{16}$$

meaning that the limit $\mu \to +\infty$ imposes the fixed (Dirichlet) boundary condition $\Phi^{(0)}_{(j,k)}(L) = 0$ for scattering states and the case of $\mu = 0$ imposes the open (Neuman) boundary condition at the end $x^{(0)} = L$ of the finite region $\mathcal{L}^{(0)}$. It is important to note that the open boundary case $\mu = 0$ and the fixed boundary case $\mu \to +\infty$ can also describe states in the quantum network consisting of a finite lead with a length $2L$ whose *both* sides are connected to N multiple semi-infinite leads, as shown in Fig. 2. Here, the open boundary case $\mu = 0$ (the fixed boundary case $\mu \to +\infty$) corresponds to the quantum state described by the wave function with the inversion symmetry (antisymmetry) at the center of the finite region with the length $2L$ in such a system.

From Eqs. (11), (12), and (14) the coefficient $b^{(n)}_{(j,k)}$ is given by

$$b^{(0)}_{(j,k)} = \frac{2\sum_{n'=1}^{N} a^{(n')}_{(j,k)}}{N+1+i\frac{\lambda}{k} + \left(N-1+i\frac{\lambda}{k}\right)\frac{1+i\frac{\mu}{k}}{1-i\frac{\mu}{k}} e^{2ikL}}, \tag{17}$$

$$b^{(\eta)}_{(j,k)} = -a^{(\eta)}_{(j,k)} + \frac{2\left(1+\frac{1+i\frac{\mu}{k}}{1-i\frac{\mu}{k}} e^{2ikL}\right)\sum_{n'=1}^{N} a^{(n')}_{(j,k)}}{N+1+i\frac{\lambda}{k} + \left(N-1+i\frac{\lambda}{k}\right)\frac{1+i\frac{\mu}{k}}{1-i\frac{\mu}{k}} e^{2ikL}} \tag{18}$$

for $\eta = 1,\dots,N$. Equations (14), (17), and (18) shows that the coefficients $a^{(0)}_{(j,k)}$ and $b^{(n)}_{(j,k)}$, $n = 0,\dots,N$ are given from the coefficients $a^{(n)}_{(j,k)}$, $n = 1,\dots,N$. We can still take any value for $a^{(n)}_{(j,k)}$, $n = 1,\dots,N$, as the N incident wave amplitudes from infinite regions $x^{(n)} \to +\infty$, $n = 1,\dots,N$, and this arbitrariness leads to necessity of the suffix j to distinguish degeneracy of the energy eigenstates $\Phi^{(n)}_{(j,k)}(x)$ corresponding to the energy E_k. In this paper, we introduce $a^{(n)}_{(j,k)}$ as

$$a^{(n)}_{(j,k)} \equiv \varsigma_j \delta_{jn} \tag{19}$$

for $n = 1,2,\ldots,N$ with a constant ς_j. Equation (19) means that the state $\Phi^{(n)}_{(j,k)}(x)$ is the scattering state produced by the incident wave from the infinite region $x^{(j)} \to +\infty$ of $\mathcal{L}^{(j)}$ only.

We define the inner products

$$\begin{aligned}\langle X|Y\rangle &\equiv \lim_{\epsilon\to+0}\int_\epsilon^L dx\ X^{(0)}(x)^* Y^{(0)}(x) \\ &\quad + \lim_{\epsilon\to+0}\sum_{n=1}^N \int_\epsilon^{+\infty} dx\ X^{(n)}(x)^* Y^{(n)}(x) \\ &= \sum_{n=0}^N \int_{\mathcal{L}^{(n)}} dx\ X^{(n)}(x)^* Y^{(n)}(x)\end{aligned} \tag{20}$$

for any quantum states X and Y, whose values at the position x in the region $\mathcal{L}^{(n)}$ are given by $X^{(n)}(x)$ and $Y^{(n)}(x)$, respectively. Here, X^* with the asterisk denotes the complex conjugate of X for any complex number X. For this inner product (20) it is essential to note that the scattering state $\Phi^{(n)}_{(j,k)}(x)$ satisfies the orthogonal relation

$$\langle \Phi_{(j,k)}|\Phi_{(j',k')}\rangle = \delta_{jj'}\delta(k-k') \tag{21}$$

for $kk' > 0$. Here, we specified the constant ς_j in Eq. (19) as

$$\varsigma_j \equiv \frac{1}{\sqrt{2\pi}} \tag{22}$$

independently with respect to the suffix $j = 1,2,\ldots,N$, so the coefficient of the term $\delta_{jj'}\delta(k-k')$ in the right-hand side of Eq. (21) becomes 1. The proof of Eq. (21) is given in Appendix B.

C. Propagator and the time evolution of wave function

Now, we assume that the initial quantum state $\Psi(0)$ at $t = 0$ is expanded in the scattering states, as

$$\Psi^{(n)}(x,0) = \sum_{j=1}^N \int_0^{+\infty} dk\ A_{(j,k)} \Phi^{(n)}_{(j,k)}(x) \tag{23}$$

at the position x in $\mathcal{L}^{(n)}$ with a constant $A_{(j,k)}$. From Eqs. (20), (21), and (23) the constant $A_{(j,k)}$ is expressed as

$$A_{(j,k)} = \langle \Phi_{(j,k)}|\Psi(0)\rangle \tag{24}$$

for $k > 0$. The initial condition (23) implies that the initial state $\Psi(0)$ does not include bound states with a discretized energy spectrum which are orthogonal to the scattering states [49].

The wave function of the system at time $t > 0$ is given by applying the time-evolutional operator $\exp(-i\hat{H}t/\hbar)$ with the Hamiltonian operator $\hat{H}$ to the initial state (23), and we obtain

$$\begin{aligned}\Psi^{(n)}(x,t) &= \sum_{j=1}^N \int_0^{+\infty} dk\ A_{(j,k)} e^{-iE_k t/\hbar} \Phi^{(n)}_{(j,k)}(x) \\ &= \sum_{n'=0}^N \int_{\mathcal{L}^{(n')}} dx'\ K^{(n,n')}(x,x';t)\Psi^{(n')}(x',0)\end{aligned} \tag{25}$$

from Eqs. (20) and (24) and $\hat{H}\Phi^{(n)}_{(j,k)}(x) = E_k \Phi^{(n)}_{(j,k)}(x)$. Here, the integral kernel $K^{(n,n')}(x,x';t)$ is called the propagator [50, 51] and is given by

$$K^{(n,n')}(x,x';t) \equiv \sum_{j=1}^N \int_0^{+\infty} dk\ \Phi^{(n)}_{(j,k)}(x)\Phi^{(n')}_{(j,k)}(x')^* e^{-iE_k t/\hbar}. \tag{26}$$

In other words, we can calculate the propagator (26) via the scattering state (10) with the coefficients (14), (17), (18), and (19), leading to the wave function at time t from Eq. (25).

III. ESCAPE BEHAVIOR OF A PARTICLE VIA MULTIPLE LEADS

A. Quantum escapes in a network system

In this section we consider the behavior of a particle that escapes from the finite region $\mathcal{L}^{(0)}$ to the semi-infinite regions $\mathcal{L}^{(n)}$, $n = 1,2,\ldots,N$. In order to discuss such phenomena, we set the initial wave function at $t = 0$ to take nonzero value only in the finite region $\mathcal{L}^{(0)}$, i.e.,

$$\Psi^{(n)}(x,0) = 0 \quad \text{for}\ \ n = 1,\ldots,N. \tag{27}$$

From Eqs. (25) and (27) the wave function $\Psi^{(0)}(x,t)$ in the region $\mathcal{L}^{(0)}$ at time t is expressed as

$$\Psi^{(0)}(x,t) = \int_0^L dx'\ K^{(0,0)}(x,x';t)\Psi^{(0)}(x',0) \tag{28}$$

by using the functions $K^{(0,0)}(x,x';t)$ and $\Psi^{(0)}(x',0)$ for this finite region only.

As shown in Appendix C, the propagator $K^{(0,0)}(x,x';t)$ is expressed as

$$K^{(0,0)}(x,x';t) = \int_{-\infty}^{+\infty} dk\ F(x,x';k)e^{-i\tau_t k^2}. \tag{29}$$

with τ_t defined by

$$\tau_t \equiv \frac{\hbar t}{2m}. \tag{30}$$

Here, $F(x,x';k)$ is defined by

$$F(x,x';k) \equiv \frac{2N}{\pi C(k)}\left\{\cos[k(x-x')] + \frac{\left(1-\frac{\mu^2}{k^2}\right)\cos[k(x+x'-2L)] + 2\frac{\mu}{k}\sin[k(x+x'-2L)]}{1+\frac{\mu^2}{k^2}}\right\} \tag{31}$$

with

$$C(k) \equiv \left| N+1+i\frac{\lambda}{k}+\left(N-1+i\frac{\lambda}{k}\right)\frac{1+i\frac{\mu}{k}}{1-i\frac{\mu}{k}}e^{2ikL}\right|^2. \quad (32)$$

It may be noted that the integral region of wave number k in the right-hand side of Eq. (29) is $(-\infty,+\infty)$, which is different from in the right-hand side of Eq. (26).

Noting that the function (31) is an even function of k, we expand it as

$$F(x,x';k) = \sum_{\nu=0}^{+\infty} B_\nu(x,x')k^{2\nu} \quad (33)$$

with respect to k^2, where $B_\nu(x,x')$ is a function of x and x' and is independent of k. Then, for $t > 0$ the k integral in Eq. (29) can be carried out, and we obtain

$$K^{(0,0)}(x,x';t) = \sum_{\nu=0}^{+\infty} B_\nu(x,x')\frac{(2\nu)!}{2^{2\nu}\nu!}\frac{1-i}{i^\nu}\sqrt{\frac{\pi}{2\tau_t^{2\nu+1}}}, \quad (34)$$

noting $0! \equiv 1$. Here we used the integral formula

$$\int_{-\infty}^{+\infty} dk\, k^{2\nu}e^{-i\tau_t k^2} = \frac{(2\nu)!}{2^{2\nu}\nu!}\frac{1-i}{i^\nu}\sqrt{\frac{\pi}{2\tau_t^{2\nu+1}}} \quad (35)$$

for $\nu = 0,1,\ldots$, which is derived from the τ_t derivative of the equation $\int_{-\infty}^{+\infty} dk\, e^{-i\tau_t k^2} = (1-i)\sqrt{\pi/(2\tau_t)}$ for $t > 0$ [52]. Equation (34) is an asymptotic expansion of the propagator $K^{(0,0)}(x,x';t)$ with respect to $1/t^{\nu+1/2}$, $\nu = 0,1,\ldots$.

Under the initial condition (27) we describe the escape behavior of a particle from the finite region $\mathcal{L}^{(0)}$. As an example of quantities that characterize such escape behavior, we consider the quantity $P(t)$ defined by

$$P(t) \equiv \frac{\int_0^L dx\, \rho^{(0)}(x,t)}{\int_0^L dx\, \rho^{(0)}(x,0)}. \quad (36)$$

This is the ratio for a particle to survive in the finite region $\mathcal{L}^{(0)}$ at time t in comparison with that at the initial time $t = 0$ [53], and we call this probability $P(t)$ the survival probability in this paper [54]. As another quantity to characterize particle escape behaviors we also consider the local velocity for the particle to escape from the finite region $\mathcal{L}^{(0)}$, which is defined by

$$V(t) \equiv \frac{\lim_{x\to+0}\sum_{n=1}^N \rho^{(n)}(x,t)v^{(n)}(x,t)}{\rho(0,t)} = -\lim_{x\to+0} v^{(0)}(x,t) \quad (37)$$

with the probability density $\rho(0,t) \equiv |\Psi(0,t)|^2$ at the junction O. Here, we used Eq. (5), and $\rho(0,t) = \lim_{x\to+0}\rho^{(1)}(x,t) = \lim_{x\to+0}\rho^{(2)}(x,t) = \cdots = \lim_{x\to+0}\rho^{(N)}(x,t)$ from Eqs. (1) and (4) to derive the second equation in the right-hand side of Eq. (37) from its first equation. We call this velocity $V(t)$ the "escape velocity" in this paper. The survival probability (36) and the escape velocity (37) can be calculated from the wave function (28) only in the finite region $\mathcal{L}^{(0)}$ via the propagator (29) or (34), without information on the particle in the semi-infinite region $\mathcal{L}^{(n)}$, $n = 1,2,\ldots,N$.

In the following subsection, we consider properties of the survival probability $P(t)$ and the escape velocity $V(t)$ mainly in the fixed boundary case $\mu \to +\infty$, while we give some analytical arguments for $P(t)$ and $V(t)$ in the open boundary case $\mu = 0$ in Appendix D.

B. Asymptotic properties of particle escapes

In the fixed boundary case $\mu \to +\infty$, the function (31) is represented as

$$F(x,x';k) = \frac{4N}{\pi}\frac{\sin[k(x-L)]\sin[k(x'-L)]}{C(k)}, \quad (38)$$

where $C(k)$ is given by

$$C(k) = \left[N+1-(N-1)\cos(2kL)+\lambda\frac{\sin(2kL)}{k}\right]^2 + \left[(N-1)\sin(2kL)-\lambda\frac{1-\cos(2kL)}{k}\right]^2. \quad (39)$$

The expansion of the function (38) with respect to k^2 as in Eq. (33) differs for the cases where $\lambda L \neq -1$ and $\lambda L = -1$, so we consider these two cases separately below.

1. Fixed boundary case with $\lambda L \neq -1$

First, we consider the case of $\lambda L \neq -1$. For the function (38), the quantity $B_\nu(x,x')$ as the coefficients of the function $F(x,x';k)$ with respect to $k^{2\nu}$ in Eq. (33) is given by

$$B_0(x,x') = 0, \quad (40)$$

$$B_1(x,x') = \frac{N(x-L)(x'-L)}{\pi(1+\lambda L)^2}, \quad (41)$$

$$B_2(x,x') = -\frac{N(x-L)(x'-L)}{6\pi(1+\lambda L)^2}\left[(x-L)^2+(x'-L)^2 + 2L^2\frac{3(N^2-1)-\lambda L(\lambda L+4)}{(1+\lambda L)^2}\right],\ldots, \quad (42)$$

concretely. By inserting these coefficients $B_\nu(x,x')$, $\nu = 0,1,\ldots$ into the formula (34) and using Eq. (28), we obtain the wave function $\Psi^{(0)}(x,t)$ in $\mathcal{L}^{(0)}$ for $t > 0$ as

$$\Psi^{(0)}(x,t) = -\frac{N(x-L)(1+i)\Theta_1}{2\sqrt{2\pi}(1+\lambda L)^2}\frac{1}{\tau_t^{3/2}} + \frac{N(x-L)(1-i)}{8\sqrt{2\pi}(1+\lambda L)^2} \times \frac{1}{\tau_t^{5/2}}\left[(x-L)^2\Theta_1+\Theta_3 + 2L^2\frac{3(N^2-1)-\lambda L(\lambda L+4)}{(1+\lambda L)^2}\Theta_1\right] + \cdots, \quad (43)$$

where Θ_ν is defined by

$$\Theta_\nu \equiv \int_0^L dx\,(x-L)^\nu\Psi^{(0)}(x,0). \quad (44)$$

Equation (43) is the wave function for the fixed boundary case $\mu \to +\infty$ with $\lambda L \neq -1$ as an expansion of $1/t^{\nu+1/2}$, $\nu = 1,2,\ldots$.

From Eqs. (1), (30), and (43) the survival probability (36) at long times is expressed asymptotically as

$$P(t) \overset{t\to+\infty}{\sim} \frac{2N^2\Xi_1}{3\pi(1+\lambda L)^4}\left(\frac{mL}{\hbar t}\right)^3 \quad (45)$$

with the constant $\Xi_1 \equiv \Theta_1^2/\int_0^L dx\, \rho^{(0)}(x,0)$ determined by the initial wave function $\Psi^{(0)}(x,0)$ only. Equation (45) means that the survival probability $P(t)$ decays asymptotically as a power of time as $\sim t^{-3}$. Moreover, from Eq. (45) we obtain

$$\lim_{t\to+\infty} \frac{P(t)}{P(t)|_{\lambda=0}} = \frac{1}{(1+\lambda L)^4}, \tag{46}$$

$$\lim_{t\to+\infty} \frac{P(t)}{P(t)|_{N=1}} = N^2, \tag{47}$$

as far as the initial wave function $\Psi^{(0)}(x,0)$ is independent of λ and N. Equation (46) shows that the probability for a particle to stay in the finite region $\mathcal{L}^{(0)}$ becomes lower for a larger potential barrier amplitude (7) at the junction O in the long time limit, and this (rather counterintuitive) result, as well as the asymptotic power decay $\sim t^{-3}$ of $P(t)$, has already been shown for the one-lead case $N = 1$ in Ref. [20]. On the other hand, Eq. (47) means that the probability for a particle to stay in the finite region $\mathcal{L}^{(0)}$ for multi semi-infinite leads becomes N^2 times higher than that for a single lead.

The first nonzero contribution to the survival probability $P(t)$ after a long time comes from the first term of the right-hand side of Eq. (43). In contrast, the escape velocity $V(t)$ is an example of quantities in which a first nonzero contribution after a long time comes from the second term of the right-hand side of Eq. (43). Actually, by inserting the right-hand side of Eq. (43) up to its second term into Eq. (3), and using Eq. (30), we obtain

$$v^{(0)}(x,t) \overset{t\to+\infty}{\sim} -\frac{L-x}{t} \tag{48}$$

asymptotically in time. Therefore, after a long time the escape velocity (37) is represented as

$$V(t) \overset{t\to+\infty}{\sim} \frac{L}{t}, \tag{49}$$

meaning that, asymptotically in time, the escape velocity $V(t)$ decays as a power $\sim t^{-1}$ and is independent of the number of semi-infinite leads, the constant λ, and the initial wave function $\Psi^{(0)}(x,0)$, and so on. The velocity (49) can be regarded as a constant velocity by which a classical mechanical particle in an ideal wire remains inside a finite region with the length L within the time interval t without an escape.

2. Fixed boundary case with $\lambda L = -1$

Next, we consider the case of $\lambda L = -1$, in which the quantities $B_\nu(x,x')$, $\nu = 0,1,\ldots$ are represented as

$$B_0(x,x') = \frac{(x-L)(x'-L)}{\pi N L^2}, \tag{50}$$

$$B_1(x,x') = -\frac{(x-L)(x'-L)}{6\pi N L^2} \times \left[(x-L)^2 + (x'-L)^2 - \frac{2L^2}{3}\frac{3N^2-1}{N^2}\right], \ldots, \tag{51}$$

concretely, from Eqs. (33), (38), and (39). By inserting these coefficients $B_\nu(x,x')$, $\nu = 0,1,\ldots$ of the function $F(x,x';t)$ with respect to k^2 into Eq. (34), the wave function (28) in the region $\mathcal{L}^{(0)}$ for $t > 0$ is represented as

$$\Psi^{(0)}(x,t) = \frac{(x-L)(1-i)\Theta_1}{\sqrt{2\pi} N L^2}\frac{1}{\tau_t^{1/2}} + \frac{(x-L)(1+i)}{12\sqrt{2\pi} N L^2} \times \left[(x-L)^2\Theta_1 + \Theta_3 - \frac{2L^2}{3}\frac{N^2-1}{N^2}\Theta_1\right]\frac{1}{\tau_t^{3/2}} + \cdots \tag{52}$$

as an expansion with respect to $1/t^{\nu+1/2}$, $\nu = 0,1,\ldots$.

From Eqs. (1), (30), (36), and (52) we derive the survival probability

$$P(t) \overset{t\to+\infty}{\sim} \frac{2m\Xi_1}{3\pi\hbar N^2 L t} \tag{53}$$

asymptotically in time. It is important to note that the survival probability (53) for $\lambda L = -1$ decays in time as a power $\sim t^{-1}$, differing from the asymptotic power decay $\sim t^{-3}$ for $\lambda L \neq -1$ as shown in Eq. (45). This difference in the decay powers of the survival probability $P(t)$ comes from the fact that the zeroth-order term of the function of Eq. (39) with respect to k disappears in the case of $\lambda L = -1$, so the function $B_0(x,x')$ becomes nonzero as in Eq. (50). We should also note that the right-hand side of Eq. (45) for $\lambda L \neq -1$ diverges in the limit $\lambda L \to -1$. In this way, we can regard the asymptotic power decay $\sim t^{-1}$ of the survival probability $P(t)$ for $\lambda L = -1$, differing from that for $\lambda L \neq -1$ as a resonance. (This kind of resonance occurs in the case of $\lambda = 0$ for the open boundary case $\mu = 0$, as shown in Appendix D). From the asymptotic form (53) of the survival probability we obtain

$$\lim_{t\to+\infty} \frac{P(t)}{P(t)|_{N=1}} = \frac{1}{N^2} \tag{54}$$

for the N-independent initial wave function $\Psi^{(0)}(x,0)$. Equation (54) indicates that by connecting more leads to the finite region $\mathcal{L}^{(0)}$, the probability of a particle to stay in the region $\mathcal{L}^{(0)}$ for $\lambda L = -1$ becomes lower after a long time, in constrast to Eq. (47) for $\lambda L \neq -1$.

From Eqs. (3), (30), and (52) we derive the local velocity $v^{(0)}(x,t)$ in $\mathcal{L}^{(0)}$ as

$$v^{(0)}(x,t) \overset{t\to+\infty}{\sim} -\frac{L-x}{3t} \tag{55}$$

asymptotically in time. Therefore, we obtain the escape velocity (37) as

$$V(t) \overset{t\to+\infty}{\sim} \frac{L}{3t} \tag{56}$$

after a long time. Equation (56) shows that the escape velocity $V(t)$ for $\lambda L = -1$ decays asymptotically in the same power $\sim t^{-1}$ as in Eq. (49) for $\lambda L \neq -1$, although its prefactor $L/3$ is one-third that in the case of $\lambda L \neq -1$.

C. Finite-time properties of particle escapes

In this subsection, we consider the finite-time behavior of particle escapes in the fixed boundary case $\mu \to +\infty$ by calculating the wave function $\Psi^{(0)}(x,t)$ numerically. In order to calculate the wave function $\Psi^{(0)}(x,t)$ concretely for the fixed

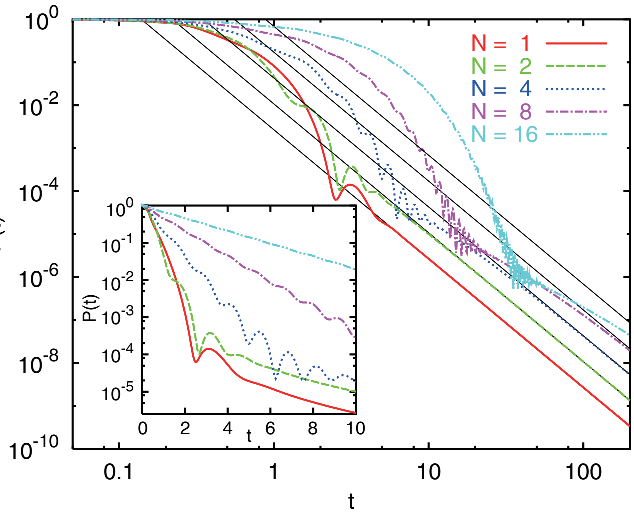

FIG. 3. (Color online) The survival probabilities $P(t)$ as functions of t for the fixed boundary case with $\lambda L \neq -1$ for $N = 1$ (the solid red line), 2 (the dashed green line), 4 (the dotted blue line), 8 (the dash-dotted purple line), and 16 (the dash-double-dotted cyan line). The main figure is log-log plots of $P(t)$ with the corresponding asymptotic power decays shown in thin straight lines, and the inset is their linear-log plots at short times. Here, and in all figures hereafter, we use dimensionless units with $L = 1$, $m = 1$, and $\hbar = 1$.

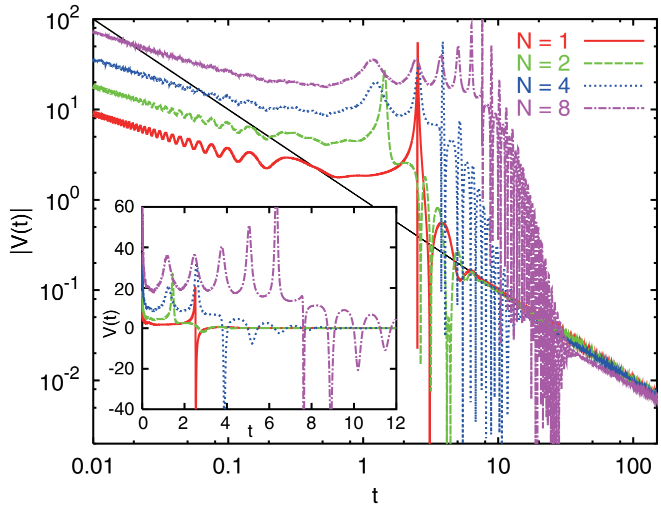

FIG. 4. (Color online) The absolute values $|V(t)|$ of escape velocities as functions of t for the fixed boundary case with $\lambda L \neq -1$ for $N = 1$ (the solid red line), 2 (the dashed green line), 4 (the dotted blue line), and 8 (the dash-dotted purple line). The main figure is log-log plots of $|V(t)|$ with a thin straight line for the asymptotic power decay, and the inset is linear-linear plots of the escape velocities $V(t)$ themselves at short times.

boundary case, we specify the initial wave function in the finite region $\mathcal{L}^{(0)}$ as

$$\Psi^{(0)}(x,0) = \sqrt{\frac{2}{L}} \sin\left(\frac{\sigma\pi}{L}x\right), \tag{57}$$

which is the σ-th eigenstate of a particle confined in the finite region $\mathcal{L}^{(0)}$ without semi-infinite leads ($\sigma = 1,2,\ldots$) [55]. Under the initial condition of Eqs. (27) and (57), from Eqs. (28), (29), and (38) the wave function $\Psi^{(0)}(x,t)$ in the finite region $\mathcal{L}^{(0)}$ at time t is represented as

$$\Psi^{(0)}(x,t) = 8\sigma N\sqrt{2L}\int_0^{+\infty} dk\, \frac{e^{-i\tau_t k^2}\sin(kL)\sin[k(x-L)]}{C(k)[(kL)^2-(\sigma\pi)^2]}, \tag{58}$$

with $C(k)$ given by Eq. (39). By carrying out the integral (58) with respect to k numerically, we calculate the survival probability $P(t)$ and the escape velocity $V(t)$ at a finite time t. In this subsection we chose the parameter values as $L = 1$, $\sigma = 1$, $m = 1$, and $\hbar = 1$.

1. Fixed boundary case with $\lambda L \neq -1$

Figure 3 is the survival probabilities $P(t)$ as functions of time t for the fixed boundary case $\mu \to +\infty$ with $\lambda L \neq -1$ under the initial wave function (57) for different numbers $N =$ 1 (the solid red line), 2 (the dashed green line), 4 (the dotted blue line), 8 (the dash-dotted purple line), and 16 (the dash-double-dotted cyan line) of semi-infinite leads. Here, we used the parameter value $\lambda = 1$, and the thin straight lines in this figure show the asymptotic power decay (45) of the survival probability for each value of N.

The main figure of Fig. 3 as log-log plots of $P(t)$ shows that the survival probability $P(t)$ approaches a power decay (45) asymptotically in time. Such an approach of the probability $P(t)$ to the corresponding power decay occurs at later times as the number of leads increases. [Therefore, the probability $P(t)$ for $N = 16$ in Fig. 3 should also approach the power decay (45) at much later times than at those in this figure.] We can also see in the inset of Fig. 3 as the linear-log plots of $P(t)$ that, at short times, the survival probability $P(t)$ decays exponentially $\sim\exp(-\alpha t)$ in time with a positive constant α, as shown especially in the cases of $N = 4$, 8, and 16. The time period for such an exponential decay of $P(t)$ is longer for more leads, and its decay rate α is smaller for more leads. One may notice that the survival probability does not decrease monotonously in time and shows a time oscillation between its exponential decay region and the power decay region. As a tendency, the survival probability $P(t)$ is higher for more leads, although there are temporal exceptions for it by its time-oscillatory behavior.

Figure 4 gives plots of the absolute values $|V(t)|$ of the escape velocities as the main figure, as well as the escape velocities $V(t)$ themselves as the inset, as functions of time t for the fixed boundary case under the initial wave function (57) for the different numbers of leads $N = 1$ (the solid red line), 2 (the dashed green line), 4 (the dotted blue line), and 8 (the dash-dotted purple line). Here, we used the parameter value $\lambda = 1$, and the thin straight line is the asymptotic power decay (49) of the escape velocity.

It is shown in the inset of Fig. 4 that at short times the escape velocity $V(t)$ oscillates in time, rather than a simple decay, and can even sometimes take a negative value. Such a time-oscillatory behavior of $V(t)$ continues for a longer time for more leads, although its time-oscillating period seems to be almost independent of N. At short times, the magnitude of the escape velocity $V(t)$ tends to increase for more leads. For some values of N, such as for $N = 1$ in the inset of

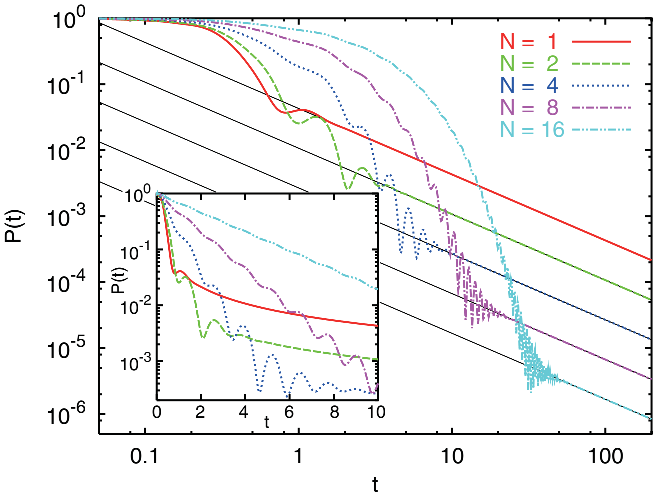

FIG. 5. (Color online) The survival probabilities $P(t)$ as functions of t for the fixed boundary case with $\lambda L = -1$ for $N = 1$ (the solid red line), 2 (the dashed green line), 4 (the dotted blue line), 8 (the dash-dotted purple line), and 16 (the dash-double-dotted cyan line). The main figure is log-log plots of $P(t)$ with the corresponding asymptotic power decays shown in thin straight lines, and the inset is their linear-log plots at short times.

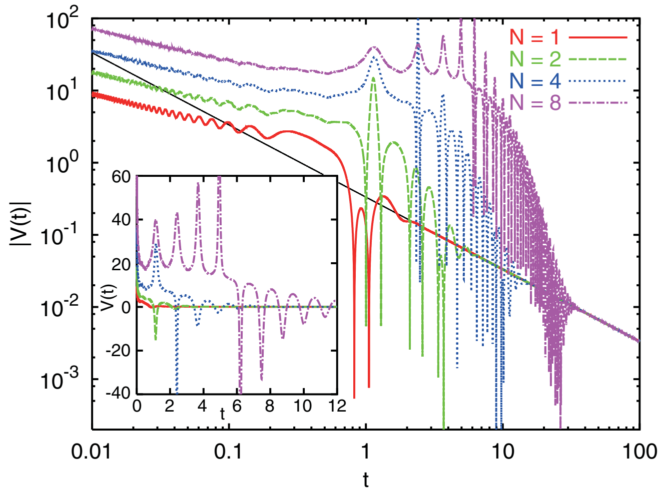

FIG. 6. (Color online) The absolute values $|V(t)|$ of the escape velocities as functions of time t for the fixed boundary case with $\lambda L = -1$ for $N = 1$ (the solid red line), 2 (the dashed green line), 4 (the dotted blue line), and 8 (the dash-dotted purple line). The main figure is log-log plots of $|V(t)|$ with a straight line for the asymptotic power decay, and the inset is linear-linear plots of the escape velocities $V(t)$ themselves at short times.

Fig. 4, a very rapid (but not abrupt) change of the escape velocity $V(t)$ from a positive value to the first negative value as a function of t occurs, when the value of $|\Psi^{(0)}(+0,t)|$ is nonzero but very small at the time t, satisfying the condition $\partial\Psi^{(0)}(x,t)/\partial x|_{x=+0} = 0$. (Note that time oscillations of $V(t)$ around the time $t \approx 10$ in the main figure of Fig. 4 look to be cut off in the middle occasionally, because of insufficient calculation points there, but they actually reach the value of zero by crossing the line $V = 0$.) After such a time oscillation, the escape velocity $V(t)$ converges rapidly to its asymptotic power decay (49), which is independent of N.

2. *Fixed boundary case with* $\lambda L = -1$

We now consider finite-time properties of particle escapes for $\lambda L = -1$ (so $\lambda = -1$ because of $L = 1$) in the fixed boundary case $\mu \to +\infty$. Figure 5 is the survival probabilities $P(t)$ as functions of time t for $N = 1$ (the solid red line), 2 (the dashed green line), 4 (the dotted blue line), 8 (the dash-dotted purple line), and 16 (the dash-double-dotted cyan line). The thin straight lines in this figure show the asymptotic power decay (53) of $P(t)$ for each value of N.

As shown in the inset of Fig. 5 as the linear-log plots of $P(t)$, especially for large $N = 8$ and 16, at short times the survival probability $P(t)$ decays exponentially in time. Such an exponential decay continues for a longer time for more attached leads, and its decay rate is smaller for more leads. After the exponential decay, the survival probability $P(t)$ shows a time-oscillatory behavior and then converges to its asymptotic power decay (53), as shown in the main figure of Fig. 5 as the log-log plots of $P(t)$. In contrast with the case where $\lambda L \neq -1$, the survival probability $P(t)$ becomes lower for larger N in this asymptotic power decay region, while it is opposite in the exponential time-decay region.

Figure 6 is the absolute values $|V(t)|$ of the escape velocities as the main figure, as well as the escape velocities $V(t)$ themselves in the inset, as functions of time t for the fixed boundary condition with $\lambda L = -1$ in the case of $N = 1$ (the solid red line), 2 (the dashed green line), 4 (the dotted blue line), and 8 (the dash-dotted purple line). The thin straight line in this figure is the asymptotic power decay (56) of the escape velocity $V(t)$.

As shown in the inset of Fig. 6, the escape velocity $V(t)$ oscillates in time, first, as a time oscillation with positive values and then as that with positive and negative values. Such an oscillatory time region continues for a longer time for more leads, although its time oscillating period seems to be almost independent of N, and has a tendency for the absolute value $|V(t)|$ of the escape velocity to be larger for larger N for this time period. (In the main figure of Fig. 6, the time oscillations of $V(t)$ look to be cut off in a middle, because of the small number of calculation points. In the actual graphs the value of $|V(t)|$ goes to zero in a time-oscillatory region with positive and negative values.) After such a time oscillation the escape velocity $V(t)$ converges rapidly to its asymptotic power decay (56), which is independent of N.

IV. CONCLUSION AND REMARKS

In this paper, we have discussed particle escapes in an open quantum network using a theoretical scattering approach. As a concrete example with a current splitter as a feature of network systems, we considered particle escape from an end of a finite one-dimensional wire to N semi-infinite one-dimensional leads. Properties of particle escape in such a quantum network were discussed by using two kinds of quantities; one is the probability $P(t)$ for the particle to remain in the finite wire at time t, the so-called survival probability, and the other is the velocity $V(t)$ for the particle to leave the finite region, the so-called escape velocity. Here, the escape velocity $V(t)$ is introduced from the probability current, based on the equation of continuity for the particle position probability density. With a fixed boundary condition at an end of the finite lead, for the potential barrier amplitude $\Lambda \neq -\hbar^2/(2mL)$ the survival probability $P(t)$ depends on the number of attached semi-infinite leads as $\lim_{t\to+\infty} P(t)/[P(t)|_{N=1}] = N^2$ and decays as a power $\sim 1/t^3$ asymptotically in time. In contrast, for the potential barrier amplitude $\Lambda = -\hbar^2/(2mL)$ the survival probability satisfies the relation $\lim_{t\to+\infty} P(t)/[P(t)|_{N=1}] = 1/N^2$, and it decays as a power $\sim 1/t$ at long times. On the other hand, the escape velocity $V(t)$ decays like CL/t asymptotically in time with the constant C which is independent of the number of leads and the initial wave function $\Psi^{(0)}(x,0)$, and so on. It was also shown that for a finite time the survival probability $P(t)$ decays exponentially in time for a longer time with a smaller decay rate for more attached leads and shows a time-oscillatory behavior between the exponential decay time region and the power decay time region. The escape velocity $V(t)$ shows a time-oscillatory behavior for a finite time, in which as a tendency its value is higher for more attached leads with a larger amplitude of time oscillations.

We described the dynamics of an escaping particle by a quantum scattering theoretical approach. It may be noted that although the time-dependent wave function of an escaping particle is expanded by the scattering states in the open network system it is nonzero only in a finite region for a finite time and is normalizable, differing from stationary quantum scattering states caused by incident plain waves from infinitely far spatial regions. In order to construct concretely the scattering states in the open network system, it is essential to specify the boundary conditions at the junction of a finite wire and multiple leads and at another end of the finite wire. We specified these boundary conditions based on the probability current given from the equation of continuity for the particle position probability density. We imposed the conservation of this current and the continuities of the particle wave function at the junction, so the scattering matrix at the junction is unitary and the scattering states satisfy the orthogonal relation automatically. It is important to note that the condition of no net current at the terminated end of a finite wire leads to a group of boundary conditions specified by a parameter μ. In this paper we mainly considered the case of $\mu \to +\infty$, i.e., of a fixed boundary condition. However, by using the case of $\mu = 0$, i.e., of the open boundary condition, we can also discuss particle escapes from a finite one-dimensional wire whose *both* ends are connected with multiple one-dimensional semi-infinite leads. In this case, for the initial state which is antisymmetric with respect to reflection at the center of the finite region, we get the same results of the survival probability $P(t)$ and the escape velocity $V(t)$ as cases of a fixed boundary condition. In contrast, for the initial state which is symmetric with the reflection at the center of the finite region, by using the open boundary condition $\mu = 0$ we obtain $\lim_{t\to+\infty} P(t)/[P(t)|_{N=1}] = N^2$ and $V(t) \overset{t\to+\infty}{\sim} 3L/t$ for $\Lambda \neq 0$, and $\lim_{t\to+\infty} P(t)/[P(t)|_{N=1}] = 1/N^2$ and $V(t) \overset{t\to+\infty}{\sim} L/t$ for $\Lambda = 0$, in which different behaviors of $P(t)$ and $V(t)$ occur at a different value of Λ from that in the antisymmetric initial state. As a remark it may be interesting if we could clarify the physical meanings of particle escapes in the case of other values of the parameter μ, i.e., a nonzero and finite values of μ. We also note that the current used to specify these boundary conditions is the current of probability density of the particle position. In this sense, the escape velocity $V(t)$ based on this probability current at the junction is not the particle velocity itself. The uncertain principle of quantum mechanics forbids specification of the particle velocity at a specific position of the particle.

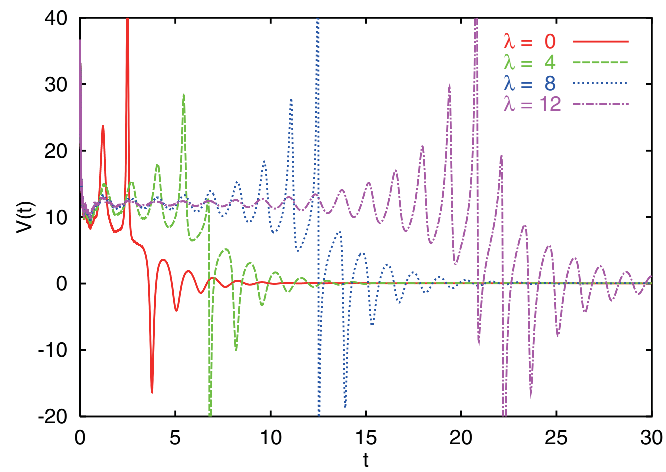

FIG. 7. (Color online) The escape velocities $V(t)$ as functions of t for the fixed boundary case with $\lambda = 0$ (the solid red line), 4 (the dashed green line), 8 (the dotted blue line), and 12 (the dash-dotted purple line).

As finite-time properties of quantum escapes, in this paper we discussed mainly dependencies of the survival probability $P(t)$ and the escape velocity $V(t)$ on the number N of attached leads, but their dependencies on other parameters also express some important escape properties. For example, the survival probability $P(t)$ decays exponentially for a finite time with a smaller decay rate for a larger value of the parameter λ proportional to the potential barrier amplitude, as known already for the case of $N = 1$ [23,26]. As another example, we show Fig. 7 for the escape velocities $V(t)$ as functions of time t for the fixed boundary case $\mu \to +\infty$ with $\lambda = 0,4,8$, and 12. Here, we chose the other parameter values as $L = 1$, $N = 4$, $\sigma = 1$, $m = 1$, and $\hbar = 1$. This figure shows that the escape velocity $V(t)$ oscillates in time around a constant value V_0 at short times, and the value V_0 is almost independent of λ but the time period appearing such time oscillations around the value V_0 becomes longer for a larger value of the parameter λ. Detailed dependencies of escape behaviors in quantum networks via multiple leads on other parameters, such as λ, μ, and σ, etc., will be discussed elsewhere.

In this paper we discussed briefly exponential decays of the survival probability for a finite time, appearing especially for a large number of attached leads as well as for a large value of the potential barrier amplitude Λ. These exponential decays would be related to the poles of the Green function or the scattering matrix [3,19–21,23,38,51]. A detailed analysis of such exponential decays of the survival probability as the scattering resonance in particle escapes via multiple leads remains as an important future problem.

ACKNOWLEDGMENTS

One of the authors (T.T.) is grateful to T. Okamura for many valuable comments and suggestions on decay behaviors in quantum open systems, and to G. P. Morriss for useful suggestions to this manuscript. He also thanks P. A. Jacquet for discussions on quantum escape problems. This research was supported by the grant sponsor: The "Open Research Project for Physical Science of Biomolecular Systems" funded by the Ministry of Education, Culture, Sports, Science, and Technology of Japan.

APPENDIX A: SCATTERING MATRIX

In this appendix we give a derivation of Eq. (11) with the scattering matrix (12).

By inserting Eq. (10) into Eq. (4) we obtain

$$a_{(j,k)}^{(0)}+b_{(j,k)}^{(0)} = a_{(j,k)}^{(1)}+b_{(j,k)}^{(1)} = \cdots = a_{(j,k)}^{(N)}+b_{(j,k)}^{(N)} = \Psi(0,t). \tag{A1}$$

On the other hand, Eqs. (6) and (10) lead to

$$\sum_{n=0}^{N}\left[a_{(j,k)}^{(n)} - b_{(j,k)}^{(n)}\right] = i\frac{\lambda}{k}\Psi(0,t). \tag{A2}$$

From Eqs. (A1) and (A2) we obtain $\sum_{n=0}^{N}[2a_{(j,k)}^{(n)} - \Psi(0,t)] = i\frac{\lambda}{k}\Psi(0,t)$, i.e.,

$$\Psi(0,t) = \frac{2}{N+1+i\frac{\lambda}{k}}\sum_{n=0}^{N}a_{(j,k)}^{(n)}. \tag{A3}$$

From Eqs. (A1) and (A3) we derive

$$\begin{aligned}\boldsymbol{b}_{(j,k)} &= \Psi(0,t)(11\cdots 1)^T - \boldsymbol{a}_{(j,k)}\\ &= S_k\boldsymbol{a}_{(j,k)}\end{aligned} \tag{A4}$$

with the scattering matrix of Eq. (12). Therefore, we obtain Eq. (11).

APPENDIX B: ORTHOGONALITY OF SCATTERING STATES

In this appendix we give a proof of the orthogonality relation (21) for the scattering state $\Phi_{(j,k)}^{(n)}(x)$.

We note the mathematical identity

$$\begin{aligned}\int_0^{+\infty} dx\ e^{ikx} &\equiv \lim_{\epsilon\to+0}\int_0^{+\infty} dx\ e^{ikx-\epsilon x}\\ &= \pi\delta(k) + i\chi(k),\end{aligned} \tag{B1}$$

where $\delta(k)$ is the δ function

$$\delta(k) = \lim_{\epsilon\to+0}\frac{1}{\pi}\frac{\epsilon}{k^2+\epsilon^2} \tag{B2}$$

and $\chi(k)$ is defined by

$$\chi(k) \equiv \lim_{\epsilon\to+0}\frac{k}{k^2+\epsilon^2}. \tag{B3}$$

Using the function (B3) we obtain

$$\begin{aligned}\int_0^{L} dx\ e^{ikx} &= (1-e^{ikL})\int_0^{+\infty} dx\ e^{ikx}\\ &= (1-e^{ikL})i\chi(k),\end{aligned} \tag{B4}$$

where we used Eq. (B1) and the identity $(1-e^{ikL})\delta(k) = 0$.

From the scattering state of Eq. (10) and the inner product from Eq. (20) for quantum states, as well as Eqs. (11), (14), (B1), and (B4), we obtain

$$\begin{aligned}\langle\,\Phi_{(j,k)}\,|\Phi_{(j',k')}\,\rangle &= \lim_{\epsilon\to+0}\int_\epsilon^L dx\ \Phi_{(j,k)}^{(0)}(x)^*\Phi_{(j',k')}^{(0)}(x) + \lim_{\epsilon\to+0}\sum_{n=1}^{N}\int_\epsilon^{+\infty} dx\ \Phi_{(j,k)}^{(n)}(x)^*\Phi_{(j',k')}^{(n)}(x)\\ &= \pi\sum_{n=1}^{N}\left[a_{(j,k)}^{(n)}{}^*a_{(j',k')}^{(n)} + b_{(j,k)}^{(n)}{}^*b_{(j',k')}^{(n)}\right]\delta(k-k') + \pi\sum_{n=1}^{N}\left[a_{(j,k)}^{(n)}{}^*b_{(j',k')}^{(n)} + b_{(j,k)}^{(n)}{}^*a_{(j',k')}^{(n)}\right]\delta(k+k')\\ &\quad - i\boldsymbol{a}_{(j,k)}^\dagger[(S_k^\dagger S_{k'} - I)\chi(k-k') + (S_k^\dagger - S_{k'})\chi(k+k')]\boldsymbol{a}_{(j',k')}\\ &\quad - ib_{(j,k)}^{(0)}{}^*[(s_k^*s_{k'}-1)\chi(k-k') + (s_k^*-s_{k'})\chi(k+k')]b_{(j',k')}^{(0)}e^{-i(k-k')L}\end{aligned} \tag{B5}$$

in which s_k is defined by

$$s_k \equiv \frac{1+i\frac{\mu}{k}}{1-i\frac{\mu}{k}}. \tag{B6}$$

Now, we note

$$\begin{aligned}\sum_{n=1}^{N}\left[a_{(j,k)}^{(n)}{}^*a_{(j',k')}^{(n)} + b_{(j,k)}^{(n)}{}^*b_{(j',k')}^{(n)}\right]\delta(k-k') &= \left[\boldsymbol{a}_{(j,k)}^\dagger\boldsymbol{a}_{(j',k')} + \boldsymbol{b}_{(j,k)}^\dagger\boldsymbol{b}_{(j',k')} - a_{(j,k)}^{(0)}{}^*a_{(j',k')}^{(0)} - b_{(j,k)}^{(0)}{}^*b_{(j',k')}^{(0)}\right]\delta(k-k')\\ &= 2\left[\boldsymbol{a}_{(j,k)}^\dagger\boldsymbol{a}_{(j',k')} - a_{(j,k)}^{(0)}{}^*a_{(j',k')}^{(0)}\right]\delta(k-k')\\ &= 2\sum_{n=1}^{N}a_{(j,k)}^{(n)}{}^*a_{(j',k')}^{(n)}\delta(k-k')\\ &= \frac{1}{\pi}\delta_{jj'}\delta(k-k')\end{aligned} \tag{B7}$$

from Eqs. (11), (13), (14), (19), and (22). Moreover, using the function of Eq. (B3), we note

$$\int dk\ \chi(k)X(k) = \hat{\mathcal{P}}\int dk\ \frac{X(k)}{k} \tag{B8}$$

for any function $X(k)$ of k, where we introduced the operator $\hat{\mathcal{P}}$ as that to take the principal integral. In this sense, for the scattering matrix (12) we obtain

$$\begin{aligned}(S_k^\dagger S_{k'} - I)\chi(k-k') + (S_k^\dagger - S_{k'})\chi(k+k')\\ = \hat{\mathcal{P}}\left[(S_k^\dagger S_{k'} - I)\frac{1}{k-k'} + (S_k^\dagger - S_{k'})\frac{1}{k+k'}\right]\\ = \mathcal{O}\end{aligned} \tag{B9}$$

with the matrix $\mathcal{O}$ whose all elements are zero. Similarly, for the quantity s_k defined by Eq. (B6) we obtain

$$\begin{aligned}(s_k^* s_{k'} - 1)\chi(k-k') + (s_k^* - s_{k'})\chi(k+k')\\ = \hat{\mathcal{P}}\left[(s_k^* s_{k'} - 1)\frac{1}{k-k'} + (s_k^* - s_{k'})\frac{1}{k+k'}\right]\\ = 0.\end{aligned} \tag{B10}$$

Inserting Eqs. (B7), (B9), and (B10) into Eq. (B5) we obtain

$$\begin{aligned}\langle\,\Phi_{(j,k)}\,|\Phi_{(j',k')}\,\rangle = \delta_{jj'}\delta(k-k') + \pi\sum_{n=1}^{N}\big[a_{(j,k)}^{(n)}{}^* b_{(j',k')}^{(n)}\\ + b_{(j,k)}^{(n)}{}^* a_{(j',k')}^{(n)}\big]\delta(k+k').\end{aligned} \tag{B11}$$

Noting that the second term of the right-hand side of Eq. (B11) is zero for $kk' > 0$, we obtain the orthogonal relation (21) of the scattering states.

APPENDIX C: PROPAGATOR $K^{(0,0)}(x,x';t)$

In this appendix we show Eq. (29).

From Eqs. (10) and (14) we note

$$\begin{aligned}\Phi_{(j,k)}^{(0)}(x)\Phi_{(j,k)}^{(0)}(x')^* &= \left|b_{(j,k)}^{(0)}\right|^2\left[e^{ik(x-L)} + \frac{1+i\frac{\mu}{k}}{1-i\frac{\mu}{k}}e^{-ik(x-L)}\right]\left[e^{-ik(x'-L)} + \frac{1-i\frac{\mu}{k}}{1+i\frac{\mu}{k}}e^{ik(x'-L)}\right]\\ &= 2\left|b_{(j,k)}^{(0)}\right|^2\left\{\cos[k(x-x')] + \mathrm{Re}\left[\frac{1-i\frac{\mu}{k}}{1+i\frac{\mu}{k}}e^{ik(x+x'-2L)}\right]\right\}\\ &= \frac{4}{\pi}\,\frac{\cos[k(x-x')] + \frac{\left(1-\frac{\mu^2}{k^2}\right)\cos[k(x+x'-2L)] + 2\frac{\mu}{k}\sin[k(x+x'-2L)]}{1+\frac{\mu^2}{k^2}}}{\left|N+1+i\frac{\lambda}{k} + \left(N-1+i\frac{\lambda}{k}\right)\frac{1+i\frac{\mu}{k}}{1-i\frac{\mu}{k}}e^{2ikL}\right|^2},\end{aligned} \tag{C1}$$

where we used Eqs. (17), (19), and (22). Here, Re$[X]$ is the real part of X for any complex number X. It is important to note that the quantity (C1) is an even function of k, namely

$$\Phi_{(j,-k)}^{(0)}(x)\Phi_{(j,-k)}^{(0)}(x')^* = \Phi_{(j,k)}^{(0)}(x)\Phi_{(j,k)}^{(0)}(x')^*. \tag{C2}$$

By inserting Eq. (C1) into Eq. (26) for $n = n' = 0$ and by noting Eq. (C2) we obtain Eq. (29) with Eqs. (30) and (31).

APPENDIX D: ESCAPE BEHAVIORS IN THE OPEN BOUNDARY CASE

In this appendix we discuss asymptotic escape behavior of a particle in the open boundary case $\mu = 0$. In this case, the function (31) is represented as

$$F(x,x';k) = \frac{4N}{\pi}\frac{\cos[k(x-L)]\cos[k(x'-L)]}{C(k)}, \tag{D1}$$

where $C(k)$ is given by

$$\begin{aligned}C(k) = \left[N+1+(N-1)\cos(2kL) - \lambda\frac{\sin(2kL)}{k}\right]^2\\ + \left[(N-1)\sin(2kL) + \lambda\frac{1+\cos(2kL)}{k}\right]^2.\end{aligned} \tag{D2}$$

In this case, the expansion of the function (D1) with respect to k^2 as in Eq. (34) differs between the cases of $\lambda = 0$ and $\lambda \neq 0$, so we discuss these two cases separately below.

1. Open boundary case with $\lambda \neq 0$

In the open boundary case $\mu = 0$ with nonzero potential barrier with $\lambda \neq 0$ at the junction O, the expansion coefficients $B_\nu(x,x')$, $\nu = 0,1,\ldots$ of the function (D1) with respect to k^2, as in Eq. (33), are represented as

$$B_0(x,x') = 0, \tag{D3}$$

$$B_1(x,x') = \frac{N}{\pi\lambda^2}, \tag{D4}$$

$$\begin{aligned}B_2(x,x') = -\frac{N}{2\pi\lambda^2}\bigg[(x-L)^2 + (x'-L)^2\\ + 2\frac{N^2 - 2\lambda L - (\lambda L)^2}{\lambda^2}\bigg],\ldots,\end{aligned} \tag{D5}$$

concretely. From the propagator of Eq. (34) with these coefficients $B_\nu(x,x')$, $\nu = 0,1,\ldots$, the wave function

[Eq. (28)] for $t > 0$ is expressed as

$$\Psi^{(0)}(x,t) = -\frac{N(1+i)\Theta_0}{2\sqrt{2\pi}\lambda^2}\frac{1}{\tau_t^{3/2}} + \frac{3N(1-i)}{8\sqrt{2\pi}\lambda^2}\left[(x-L)^2\Theta_0 + \Theta_2 + 2\frac{N^2-2\lambda L-(\lambda L)^2}{\lambda^2}\Theta_0\right]\frac{1}{\tau_t^{5/2}} + \cdots, \quad \text{(D6)}$$

with Θ_ν defined by Eq. (44).

From Eq. (D6) the survival probability $P(t)$ is represented asymptotically in time as

$$P(t) \overset{t\to+\infty}{\sim} \frac{2N^2\Xi_0 L}{\pi\lambda^4}\left(\frac{m}{\hbar t}\right)^3 \quad \text{(D7)}$$

with the constant $\Xi_0 \equiv \Theta_0^2/\int_0^L dx\, \rho^{(0)}(x,0)$ determined by the initial wave function $\Psi^{(0)}(x,0)$ only. Equation (D7) leads to the relations

$$\lim_{t\to+\infty}\frac{P(t)}{P(t)|_{N=1}} = N^2, \quad \text{(D8)}$$

$$\lim_{t\to+\infty}\frac{P(t)}{P(t)|_{\lambda=1}} = \frac{1}{\lambda^4}, \quad \text{(D9)}$$

for the N- and λ-independent initial wave function $\Psi^{(0)}(x,0)$. Therefore, the N dependence (D8) of the asymptotic survival probability for the open boundary case with $\lambda \neq 0$ is the same as that shown in Eq. (47) for $\lambda L \neq -1$ in the fixed boundary case. In contrast, the asymptotic survival probability is inversely proportional to λ^4 in Eq. (D7), while in the fixed boundary case with $\lambda L \neq -1$ it is inversely proportional to $(1+\lambda L)^4$ as shown in Eq. (45).

From Eqs. (3) and (D6) we also derive an asymptotic expression of the local velocity $v^{(0)}(x,t)$ in the finite region $\mathcal{L}^{(0)}$ as

$$v^{(0)}(x,t) \overset{t\to+\infty}{\sim} -\frac{3(L-x)}{t}. \quad \text{(D10)}$$

Therefore, the escape velocity (37) is given by

$$V(t) \overset{t\to+\infty}{\sim} \frac{3L}{t} \quad \text{(D11)}$$

asymptotically in time, meaning that the escape velocity decays as a power $\sim t^{-1}$ as in the fixed boundary case, but its value is 3 times as high as in Eq. (49).

2. Open boundary case with $\lambda = 0$

In the case of zero potential barrier with $\lambda = 0$, from Eqs. (33) and (D1) we derive the quantities $B_\nu(x,x')$, $\nu = 0,1,\ldots$ as

$$B_0(x,x') = \frac{1}{\pi N}, \quad \text{(D12)}$$

$$B_1(x,x') = -\frac{1}{2\pi N}\left[(x-L)^2 + (x'-L)^2 - 2L^2\frac{N^2-1}{N^2}\right], \ldots, \quad \text{(D13)}$$

concretely in the open boundary case $\mu = 0$. By using these coefficients $B_\nu(x,x')$, $\nu = 0,1,\ldots$ and Eqs. (28) and (34), the wave function $\Psi^{(0)}(x,t)$ for $t > 0$ in $\mathcal{L}^{(0)}$ is represented as

$$\Psi^{(0)}(x,t) = \frac{(1-i)\Theta_0}{\sqrt{2\pi}N}\frac{1}{\tau_t^{1/2}} + \frac{1+i}{4\sqrt{2\pi}N} \times\left[(x-L)^2\Theta_0 + \Theta_2 - 2L^2\frac{N^2-1}{N^2}\Theta_0\right]\frac{1}{\tau_t^{3/2}} + \cdots \quad \text{(D14)}$$

with Θ_ν defined by Eq. (44).

From Eq. (D14) the survival probability $P(t)$ is represented asymptotically in time as

$$P(t) \overset{t\to+\infty}{\sim} \frac{2\Xi_0 m L}{\pi N^2 \hbar t}. \quad \text{(D15)}$$

Equation (D15) shows that the survival probability $P(t)$ in the case of $\mu = 0$ and $\lambda = 0$ decays asymptotically as a power $\sim t^{-1}$, as in Eq. (53) for the fixed boundary case with $\lambda L = -1$. Moreover, from Eq. (D15) we derive the relation with the same as Eq. (54) for the λ- and N-independent initial wave function $\Psi^{(0)}(x,0)$.

From Eqs. (3), (30), and (D14) we derive the local velocity $v^{(0)}(x,t)$ in the finite region $\mathcal{L}^{(0)}$, which is asymptotically the same as Eq. (48) in time. Therefore, in the open boundary case with $\lambda = 0$ we obtain the same asymptotic escape probability $V(t)$ as Eq. (49).

[1] R. W. Gurney and E. U. Condon, Phys. Rev. **33**, 127 (1929).
[2] R. G. Winter, Phys. Rev. **123**, 1503 (1961).
[3] W. van Dijk and Y. Nogami, Phys. Rev. Lett. **83**, 2867 (1999); Phys. Rev. C **65**, 024608 (2002).
[4] H. A. Kramers, Physica **7**, 284 (1940).
[5] P. Hänggi, P. Talkner, and M. Borkovec, Rev. Mod. Phys. **62**, 251 (1990).
[6] N. G. van Kampen, *Stochastic Processes in Physics and Chemistry* (Elsevier, Amsterdam, 1992).
[7] W. Bauer and G. F. Bertsch, Phys. Rev. Lett. **65**, 2213 (1990); O. Legrand and D. Sornette, *ibid.* **66**, 2172 (1991); W. Bauer and G. F. Bertsch, *ibid.* **66**, 2173 (1991).
[8] H. Alt, H. -D. Gräf, H. L. Harney, R. Hofferbert, H. Rehfeld, A. Richter, and P. Schardt, Phys. Rev. E **53**, 2217 (1996).
[9] V. Paar and H. Buljan, Phys. Rev. E **62**, 4869 (2000).
[10] E. G. Altmann and T. Tél, Phys. Rev. Lett. **100**, 174101 (2008); Phys. Rev. E **79**, 016204 (2009).
[11] P. Gaspard and G. Nicolis, Phys. Rev. Lett. **65**, 1693 (1990).
[12] P. Gaspard, *Chaos, Scattering and Statistical Mechanics* (Cambridge University Press, Cambridge, 1998).
[13] R. Klages, *Microscopic Chaos, Fractals and Transport in Nonequilibrium Statistical Mechanics* (World Scientific, Singapore, 2007).

[14] V. Milner, J. L. Hanssen, W. C. Campbell, and M. G. Raizen, Phys. Rev. Lett. **86**, 1514 (2001).
[15] N. Friedman, A. Kaplan, D. Carasso, and N. Davidson, Phys. Rev. Lett. **86**, 1518 (2001).
[16] L. A. Bunimovich and C. P. Dettmann, Europhys. Lett. **80**, 40001 (2007).
[17] M. F. Demers and L.-S. Young, Nonlinearity **19**, 377 (2006).
[18] C. H. Lewenkopf and H. A. Weidenmüller, Ann. Phys. (NY) **212**, 53 (1991).
[19] G. Casati, G. Maspero, and D. L. Shepelyansky, Phys. Rev. E **56**, R6233 (1997).
[20] G. García-Calderón, I. Maldonado, and J. Villavicencio, Phys. Rev. A **76**, 012103 (2007).
[21] G. García-Calderón, AIP Conf. Proc. **1334**, 84 (2011).
[22] I. V. Zozoulenko and T. Blomquist, Phys. Rev. B **67**, 085320 (2003).
[23] D. Onley and A. Kumar, Am. J. Phys. **59**, 562 (1991).
[24] F. -M. Dittes, H. L. Harney, and A. Müller, Phys. Rev. A **45**, 701 (1992); H. L. Harney, F. -M. Dittes, and A. Müller, Ann. Phys. (NY) **220**, 159 (1992).
[25] M. Miyamoto, Phys. Rev. A **68**, 022702 (2003).
[26] T. Taniguchi and S. Sawada, Phys. Rev. E **83**, 026208 (2011).
[27] A. del Campo, Phys. Rev. A **84**, 012113 (2011).
[28] G. García-Calderón and L. G. Mendoza-Luna, Phys. Rev. A **84**, 032106 (2011).
[29] Y. Gefen, Y. Imry, and M. Ya. Azbel, Phys. Rev. Lett. **52**, 129 (1984); M. Büttiker, Y. Imry, and M. Ya. Azbel, Phys. Rev. A **30**, 1982 (1984).
[30] M. Büttiker, Phys. Rev. B **32**, 1846 (1985).
[31] W. Porod, Z. Shao, and C. S. Lent, Appl. Phys. Lett. **61**, 1350 (1992).
[32] T. Taniguchi and M. Büttiker, Phys. Rev. B **60**, 13814 (1999).
[33] B. Shapiro, Phys. Rev. Lett. **50**, 747 (1983).
[34] P. Exner and P. Šeba, Phys. Lett. A **128**, 493 (1988).
[35] S. Bandopadhyay and A. M. Jayannavar, Phys. Lett. A **335**, 266 (2005).
[36] Z. Sobirov, D. Matrasulov, K. Sabirov, S. Sawada, and K. Nakamura, Phys. Rev. E **81**, 066602 (2010).
[37] T. Kottos and U. Smilansky, Phys. Rev. Lett. **85**, 968 (2000); J. Phys. A: Math. Gen. **36**, 3501 (2003).
[38] F. Barra and P. Gaspard, Phys. Rev. E **65**, 016205 (2001).
[39] J. E. Avron and L. Sadun, Ann. Phys. (NY) **206**, 440 (1991).
[40] V. Kostrykin and R. Schrader, J. Phys. A: Math. Gen. **32**, 595 (1999).
[41] T. Taniguchi, Phys. Lett. A **279**, 81 (2001).
[42] C. Texier and G. Montambaux, J. Phys. A: Math. Gen. **34**, 10307 (2001).
[43] S. Datta, *Electronic Transport in Mesoscopic Systems* (Cambridge University Press, Cambridge, 1995).
[44] Y. Imry, *Introduction to Mesoscopic Physics* (Oxford University Press, New York, 1997).
[45] F. A. Buot, *Nonequilibrium Quantum Transport Physics in Nanosystems* (World Scientific, Singapore, 2009).
[46] The local velocity (3) is defined only at the point where the particle exists, i.e., at the point x satisfying the condition $\Psi^{(n)}(x,t) \neq 0$.
[47] At the time t satisfying the condition $\lim_{x\to+0} \Psi^{(n)}(x,t) = 0$ or $\Psi^{(0)}(L,t) = 0$, the boundary condition of Eqs. (5) or (8) is not well defined, because here the local velocity $\lim_{x\to+0} v^{(n)}(x,t)$ or $v^{(0)}(L,t)$ cannot be introduced [46]. For such a case, Eqs. (5) and (8) have to be replaced by the conditions $\lim_{x\to+0} \sum_{n=0}^{N} \mathcal{J}^{(n)}(x,t) = 0$ and $\mathcal{J}^{(0)}(L,t) = 0$ with $\mathcal{J}^{(n)}(x,t) \equiv (\hbar/m)\,\mathrm{Im}\big[\Psi^{(n)}(x,t)^{*}\partial\Psi^{(n)}(x,t)/\partial x\big] = \rho^{(n)}(x,t)v^{(n)}(x,t)$, respectively.
[48] In principle, Eqs. (5) and (8) allow the quantities μ and λ in Eqs. (6) and (9) to depend on time t, respectively, but in this paper we consider only the cases in which both of μ and λ are time-independent constants.
[49] In general, open quantum network systems may have bound states with discretized energy spectrum, which are orthogonal to scattering states [39]. Effects of such bound states in escape phenomena are discussed in Ref. [3].
[50] J. J. Sakurai and J. Napolitano, *Modern Quantum Mechanics* (Addison-Wesley, San Francisco, 1994).
[51] The function $G^{(n,n')}(x,x';t) \equiv \theta(t)K^{(n,n')}(x,x';t)$ is the retarded Green function [50]. Here, $\theta(t)$ is the step function whose value is 1 for $t > 0$ and is 0 for $t < 0$.
[52] M. R. Spiegel, *Schaum's Outline Series: Theory and Problems of Complex Variables* (McGraw-Hill, New York, 1964).
[53] In this paper we do not prove the completeness of the scattering states. Therefore, even if we introduce the initial states as the normalized one $\langle \Psi(0) \mid \Psi(0) \rangle = 1$ in general, the right-hand side of Eq. (23) with the coefficient (24) might not be normalized. We should also note that we need a different normalization factor for the systems shown schematically in Figs. 1 and 2. For these reasons we do not assume the normalization of the initial wave function in this paper, and, instead, we put the factor $1/\int_0^L dx\, \rho^{(0)}(x,0)$ in the right-hand side of Eq. (36) so we can still impose the condition $P(0) = 1$. We do not need this kind of factor for Eq. (37), because the local velocity (3) is given from the ratio $\partial\Psi^{(n)}(x,t)/\partial x/\Psi^{(n)}(x,t)$ so the prefactor of the wave function $\Psi^{(n)}(x,t)$ is canceled out in the local velocity $v^{(n)}(x,t)$.
[54] The probability for particles to remain in the initially confined region has been referred to in several different ways, such as the survival probability [14–16,22,26], the nonescape probability [3,20,25,27], and the quantum staying probability [38].
[55] The initial condition expressed by Eqs. (27) and (57) satisfies the boundary condition (4). Although for this initial condition we cannot apply the boundary conditions (5) and (8) because of $\Psi^{(n)}(+0,0) = 0$ or $\Psi^{(0)}(L,0) = 0$ [46], the modified boundary conditions $\lim_{x\to+0} \sum_{n=0}^{N} \mathcal{J}^{(n)}(x,0) = 0$ and $\mathcal{J}^{(0)}(L,0) = 0$ [47] for such a case are satisfied because of $\lim_{x\to+0} \mathcal{J}^{(n)}(x,0) = 0$ and $\mathcal{J}^{(0)}(L,0) = 0$.